Cureus Journal of Engineering

Open Access Original Article

Wideband Compact Flexible Patch Antenna Design on Polydimethylsiloxane (PDMS) for Wearable Technology

Received 04/01/2025
Review began 04/03/2025
Review ended 04/20/2025
Published 04/24/2025

DOI: https://doi.org/10.7759/s44388-025-04462-7

Md. Mehedi Hasan [1] , Abu Zafor Muhammad Touhidul Islam [1]

1. Department of Electrical and Electronic Engineering, University of Rajshahi, Rajshahi, BGD

Corresponding author: Abu Zafor Muhammad Touhidul Islam, touhid.eee@ru.ac.bd

Abstract

This paper provides the design of a wideband compact flexible rectangular slotted patch antenna on polydimethylsiloxane (PDMS) and its performance analysis for wearable applications. Rectangular slots on the patch plane and partial ground are included to improve the operational bandwidth (BW) of the antenna. The proposed antenna is designed on a flexible PDMS substrate with relative permittivity of 2.74 and loss tangent of 0.057 and optimized to a small size of 35 × 25 × 2 mm^3 using a powerful, 3D electromagnetic simulation software package (Computer Simulation Technology) studio suite to satisfy the needs of lower fifth generation, Worldwide Interoperability for Microwave Access, Wireless Fidelity, and Industrial, Scientific, and Medical band wireless applications. The proposed antenna with a microstrip line feed has two resonant frequencies at 3.5 GHz and 4.85 GHz and it operates over the frequency range of 2.53 GHz to 5.81 GHz. In free space, the antenna provides a large BW of 3.28 GHz, a maximum radiation efficiency of 85.25%, and acceptable return loss, Voltage Standing Wave Ratio, gain, directivity, and radiation characteristics over the operational frequency range. Under the on-body condition, the antenna's performance analysis, bending analysis, and Specific Absorption Rate (SAR) analysis were also performed on a body phantom model, yielding positive results with SAR values less than the recommended safety limit of 1.6 W/kg. The comparative performance analysis proves the suitability of this antenna for applications in wearable electronics.

Categories: Microwave and RF Engineering, Wireless Communication Systems
Keywords: wearable antenna, polydimethylsiloxane, wideband, flexible, 5g, phantom, specific absorption rate

Introduction

Wearable antennas have gained a lot of popularity recently due to their various potential applications in tracking, location sensing, diagnostics, and health monitoring [1]. The most common application for these antennas is in Wireless Body Area Networks (WBAN) systems; they are often positioned in different parts of the body and operate in alignment to monitor a variety of bio-signals and provide effective body-to-body communications [2,3]. The fifth generation (5G) wearable antennas provide a wide range of applications in the medical field where they used as a medium for transferring data to monitor patient's critical health conditions [4]. However, designing efficient antennas for WBAN wireless applications is challenging because of the limits on their shape, size, material properties, and radiation performance. Moreover, the close proximity of the human body, robustness, wearer's comfort, frequency detuning, and others are critical features in wearable antenna formation. Therefore, the selection of suitable materials is the key in designing an efficient wearable microstrip patch antenna. To attain the design objectives, a great deal of research has been done with various design structures including microstrip patch, electromagnetic band gap (EBG) based monopole antennas, planar monopole, vertical monopoles, fractal, Inverted-F planar, and inkjet printed photopaper-based monopole [5-12]. A small size and low-profile wearable microstrip patch antenna is designed using a vinyl polymer-based flexible substrate and the combination of the Koch fractal geometry, meandering slits, and defected ground structure to achieve a novel hybrid structure with enhanced impedance bandwidth (BW) in [5]. In [6], a fully fabric-based slotted Planar Inverted-F Antenna (PIFA) is designed for WBAN applications for the first time with high BW (more than 46%) and reasonable gain (ca. 1.5 dB). Authors in [7] performed a number of propagation measurements of belt-to-head and belt-to-wrist channels with inverted F-antennas, PIFAs, monopole, loop and dipole antennas, and derived propagation models. It was found that the channel can be separated into short-term and long-term fading components. A novel monopole antenna with an Inkjet-Printed EBG structure array on paper substrate is presented in [8] for wearable applications and demonstrated its superior performance compared to a conventional microstrip monopole antenna. Authors in [9] have performed statistical analysis and performance evaluation for on-body radio propagation with tow microstrip patch antennas for various links, and demonstrated that the human body is a major shadowing contributor in body area network radio systems. The design and performance analysis of a small size and single-layer textile Multiple Input Multiple Output antenna utilizing the theory of characteristic mode and a small ground plane as the main radiator for wearable applications were performed in [10]. The study in [11] demonstrated the design of a dual-band wearable fractal-based monopole patch antenna integrated with an EBG structure, which covers the GSM-1800 MHz and Industrial, Scientific, and Medical (ISM) 2.45 GHz bands. The EBG structure was used to reduce the radiation into the human body and the effect of frequency detuning due to the human body. Researchers in [12] have proposed numerous directional and omnidirectional wideband antennas to meet the requirements of microwave-based head imaging systems and studied the effect of directionality on image quality of those systems to cover a wide BW (1.25-2.4 GHz) used in microwave head imaging.

However, due to their various advantages, multiband and broadband antennas are becoming more popular. The medical field requires wideband antennas with a BW of at least 2 GHz or higher, and they are preferred due to their large BW and low power consumption [13]. Polydimethylsiloxane (PDMS) is a widely used substrate in research because it provides stretchability and flexibility. However, the use of a PDMS substrate integrated with conductive fabric in [14,15] and PDMS-copper foil in [16,17] limits the stretchability in their earlier designs. In [18], a PDMS-based wearable wideband antenna with the overall dimensions of 24 × 38 mm^2 was designed and simulated, which operates in the 3 GHz to 6 GHz frequency range. Although the stated antennas showed promising results for wearable applications, they have larger sizes, narrow BWs, expensive substrates, and other limitations.

The research gap in wideband flexible wearable antenna design lies in balancing the need for broad frequency operation with the constraints of flexible materials and the body-worn environment. Specifically, challenges include achieving wide BW while maintaining good performance and minimizing the Specific Absorption Rate (SAR) under various bending and deformation scenarios. In essence, the goal is to move beyond the limitations of current wearable antenna designs and create antennas that are truly compact, flexible, wideband, robust, and suitable for a wide range of applications.

Therefore, continuous advances in research are now focused on wideband, low-cost, and tiny antennas for wearable applications. This manuscript proposed a small size, low-cost, wideband wearable slotted patch antenna embedded with PDMS substrate for wearable applications. The proposed antenna is applicable for most popular lower 5G (3.33-4.2 GHz), Worldwide Interoperability for Microwave Access (WiMAX) (3.4-3.6 GHz), Wireless Fidelity (Wifi) (5.15-5.8 GHz), and ISM (5.2-5.8 GHz) frequency band applications. The Computer Simulation Technology (CST) Microwave Studio (MWS) software is used for the simulation and numerical performance analysis of the proposed wideband microstrip patch antenna.

The paper is prepared as follows. The first section offers introduction to wideband flexible and wearable patch antennas, the related works, and research objectives. The proposed antenna structure and design details are presented in "Materials & Methods" section. "Results" section presents the simulated results and performance analysis of the designed antenna under the off-body and on-body conditions, bending analysis, and SAR analysis. "Discussion" section provides performance comparison of the proposed antenna and the antenna designed in earlier studies, which is followed by a conclusion.

Materials And Methods

Antenna design methodology

The structure of the proposed antenna is illustrated in Figure *1*. It is designed and simulated by the Time Domain solver of CST MWS Professional 3D EM Software, Version 2018. The transparent, low weight, and flexible PDMS polymer is used as a substrate with a height of 2 mm, relative permittivity ε_r of 2.74, and loss tangent tan(δ) of 0.057. The patch consists of an isosceles triangle with four parallel rectangular-shaped flat bars. The antenna is excited via a microstrip feedline. Conductive silver (Ag) paste with a thickness of 0.1 mm is used to make the patch, feedline, and ground plane. A set of rectangular slots are added to the patch plane and partial ground plane, and the design parameters are optimized to improve the antenna's impedance matching and BW. The optimized, net-compact size of the antenna is 35 × 25 × 2 mm^3.

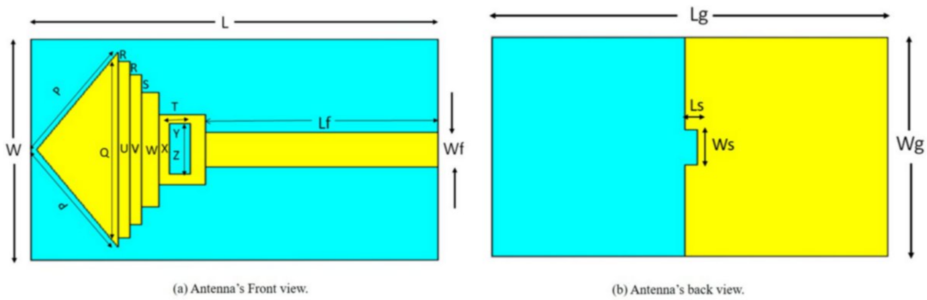

FIGURE 1: Geometry of the proposed PDMS-based flexible wideband antenna

PDMS, polydimethylsiloxane

The length and width of the PDMS substrate are chosen as 35 mm and 25 mm, respectively. As seen from the front view of Figure *1a*, the length of the base Q and leg P of the triangular part of the patch are 22 mm and 13.04 mm, respectively. The lengths (U, V, W, and X) and widths (R, R, S, and T) of four parallel rectangular-shaped flat bars of the patch are defined in Table *1*. To make sure the 50 Ω impedance matching of the antenna, the feedline's length Lf of 20 mm and width Wf of 3.96 mm are chosen. Trial-and-error analysis is used for obtaining the rectangular slot dimensions (Y × Z = 5.8 × 1.8 mm^2) on the patch plane. The area of the partial ground plane is selected as 18 × 25 mm^2 and positioned at the lowermost side of the PDMS substrate as shown in the back view of the antenna in Figure *1b*. The dimension of ground slot is taken as (Ws × Ls = 4 × 1.15 mm^2). Table *1* lists the main design parameters for the proposed antenna and their optimized values.

Parameter	Value (mm)
Ground width (Wg)	25
Ground length (Lg)	18
Ground slot dimension (Ws × Ls)	4 × 1.15
Substrate width (W)	25
Substrate length (L)	35
Base length of triangle (Q)	22
Leg length of triangle (P)	13.04
Length of parallel bar (U/V/W/X)	20/17/13/8
Width of parallel flat bar (R/R/S/T)	1/1/1.5/4
Slot dimension on patch plane (Y × Z)	5.8 × 1.8
Width of feedline (Wf)	3.96
Length of feedline (Lf)	20

TABLE 1: Design parameters of the proposed antenna

Results

The antenna's overall performance is studied both in free space (off-body) and on phantoms (on-body), as it is designed for wearable applications. This is because some of the electromagnetic energy from the antenna is absorbed and reradiated by the tissues of the human body at higher frequencies. Because of this, antenna performance parameters including resonance frequency, BW, and radiation pattern can be greatly influenced by the electromagnetic characteristics of tissues. Furthermore, various antenna parameters, including as return loss, gain, radiation patterns, and SAR, are investigated.

Off-body numerical results

Return Loss (S11)

The return loss (S11 parameter) represents the amount of power reflected back from the antenna's input port and the remaining power that the antenna radiates. In practical applications, an antenna's return loss should be less than or equal to −10 dB in order to work efficiently in a certain frequency band. The change in return loss with operating frequency of the designed antenna is shown in Figure *2*. It demonstrates that the antenna operates in the wide frequency range of 2.53 GHz to 5.81 GHz with return loss less than −10dB. The antenna exhibits two resonant peaks at 3.5 GHz and 4.85 GHz frequency where the values of return loss are −45.38 dB and −27.53 dB, respectively. The BW of the antenna is 3.28 GHz that covers most popular lower 5G (3.33-4.2 GHz), WiMAX (3.4-3.6 GHz), Wifi (5.15-5.8 GHz), and ISM (5.2-5.8GHz) frequency bands.

A microstrip patch antenna can exhibit two distinct resonant modes due to the physical characteristics of its structure, particularly when the patch is not perfectly square or rectangular, or when it has specific design features like slots or shorting pins. These multimodes arise from different current distributions across the patch and are influenced by the antenna's dimensions, material properties, and the presence of any modifying elements. In the proposed designed antenna, the two resonance modes may originate from the geometry of the antenna and the way it is excited. The antenna's triangular shape and the presence of slots introduce different resonant lengths and surface current distributions, leading to two distinct resonant frequencies. The slots also modify the effective patch length, influencing the resonant frequency.

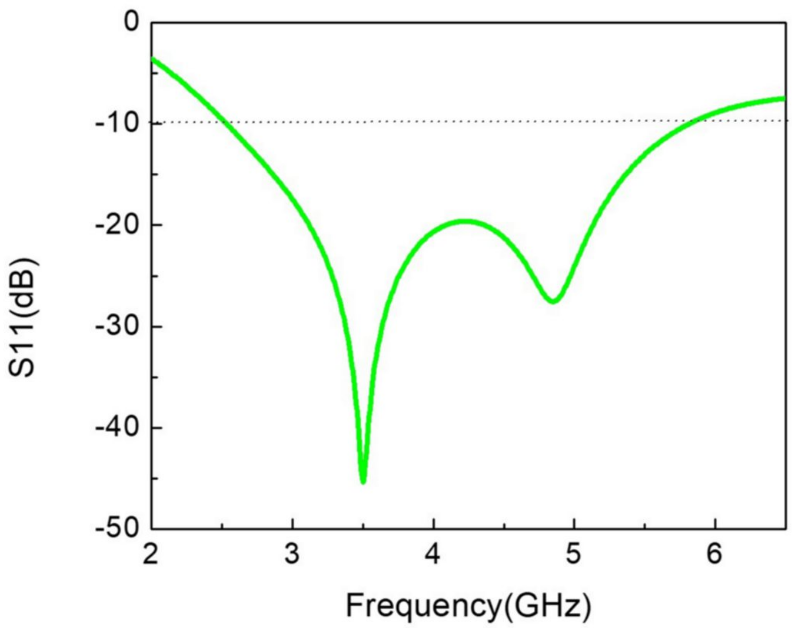

FIGURE 2: Return loss (S11) vs. frequency of the proposed antenna

Voltage Standing Wave Ratio

Voltage Standing Wave Ratio (VSWR) demonstrates the signal reflected back from the designed antenna. For a good designed antenna, VSWR should be between 1 and 2 in the operating frequency band. VSWR also define the matching of impedances to the transmission line. The proposed antenna's VSWR values at 3.5 GHz and 4.85 GHz are 1.01 and 1.22, respectively, indicating good impedance matching over the operating range of 2.53-5.81 GHz as shown in Figure *3*.

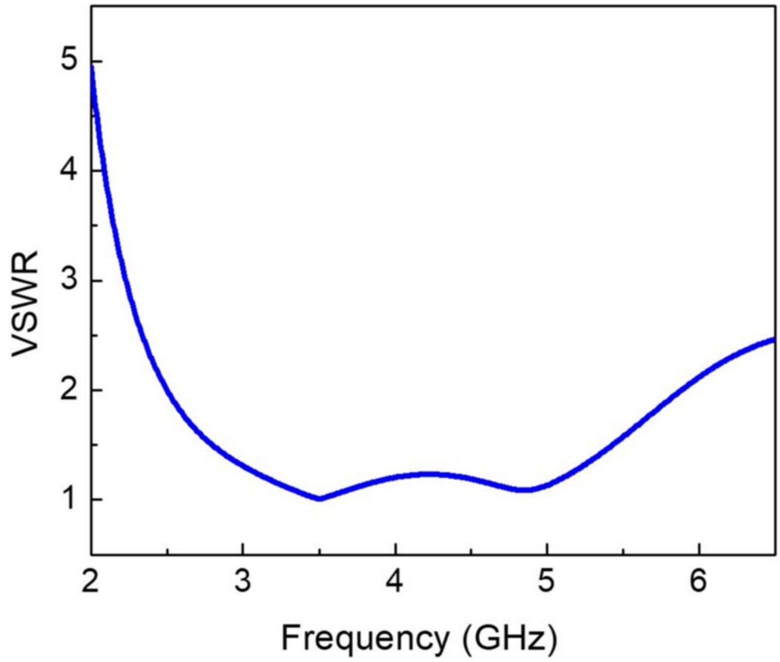

FIGURE 3: VSWR vs frequency of the proposed antenna

VSWR, Voltage Standing Wave Ratio

Gain

The gain of a transmitting antenna is the efficiency with which it transforms input power into radio waves that go in a certain direction. Figure 4 shows the proposed antenna's 3D gain at the resonant frequencies of 3.5 GHz and 4.85 GHz as well as the gain vs. frequency graph. The maximum gain of the proposed antenna is observed as 2.58 dB at 3.5 GHz (Figure 4a) and 2.8 dB at 4.85 GHz (Figure 4b). Over the antenna's operational frequency range, a maximum gain of 2.85 dB is observed (Figure 4c). The proposed antenna is thus providing reasonable gain.

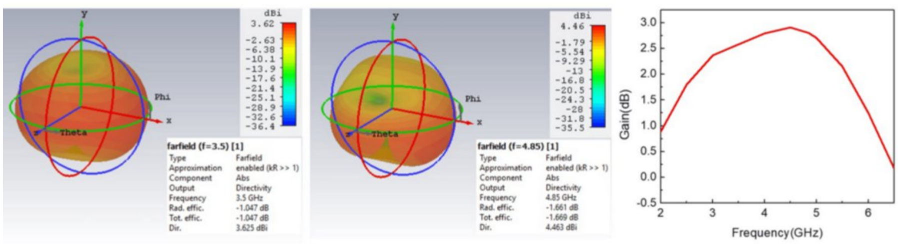

(a) 3D Gain at 3.5 GHz. (b) 3D Gain at 4.85 GHz. (c) Gain vs frequency plot.

FIGURE 4: Gain of the proposed antenna

Directivity

Figure 5 depicts the 3D directivity of the proposed antenna at the two resonant peaks of 3.5 GHz and 4.85 GHz. The maximum directivity is observed to be 3.62 dBi at 3.5 GHz (Figure 5a) and 4.46 dBi at 4.85 GHz (Figure 5b). Figure 5c illustrates the change in antenna's directivity with the operating frequency, and a maximum directivity of 4.55 dBi is observed over the range of operation of the proposed antenna.

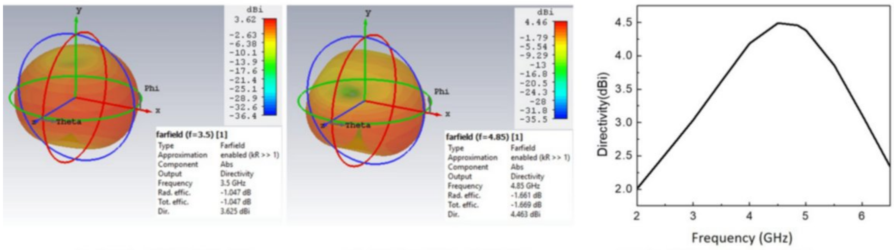

(a) 3D Directivity at 3.5 GHz. (b) 3D Directivity at 4.85 GHz. (c) Directivity vs frequency plot.

FIGURE 5: Directivity of the proposed antenna

Efficiency

The efficiency of an antenna is defined as the ratio of the radiated power to the applied total power to the antenna at a specific frequency. Figure 6 depicts the variation in radiation and total efficiency with frequency of the designed antenna. The designed antenna's simulated radiation efficiency is found to be 78.59% at 3.5 GHz and 68.54% at 4.85 GHz, with a maximum efficiency of 85.25% within the antenna's operational frequency range. The proposed antenna is thus providing reasonable efficiencies.

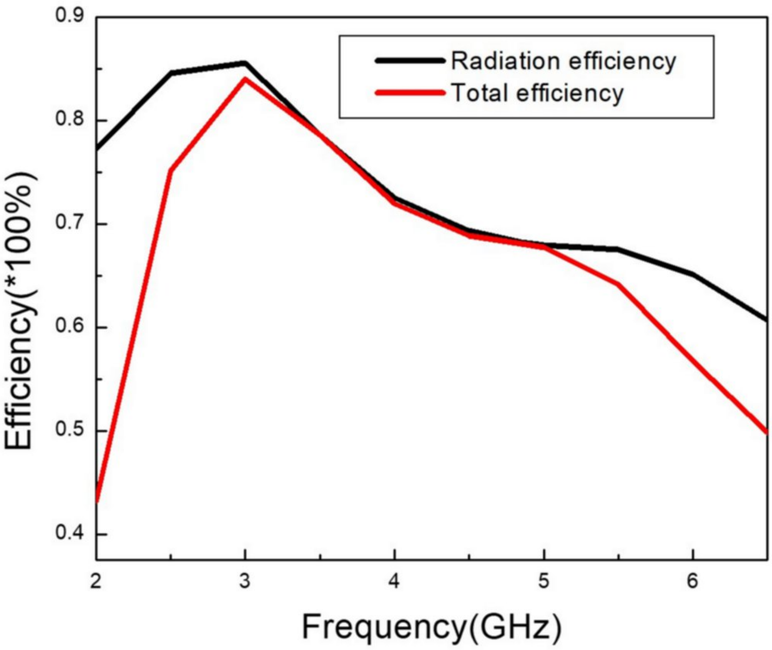

FIGURE 6: Efficiency vs. frequency of the proposed antenna

Surface Current Distribution

Surface current distribution represents the actual electric current obtained at the antenna's input port by an applied electromagnetic field. The distributions of surface current of the proposed antenna at the resonance frequencies of 3.5 GHz and 4.85 GHz are shown in Figure 7. It is evident from the figure that surface current originates from the microstrip line feed and is dispersed across the antenna, suggesting that the entire antenna plays a role in both the resonance peak frequencies. The maximum surface current densities of 47.5 A/m at 3.5 GHz (Figure 7a) and 53 A/m at 4.85 GHz (Figure 7b) are distributed along the bottom edges of the patch and lower portion of the feedline.

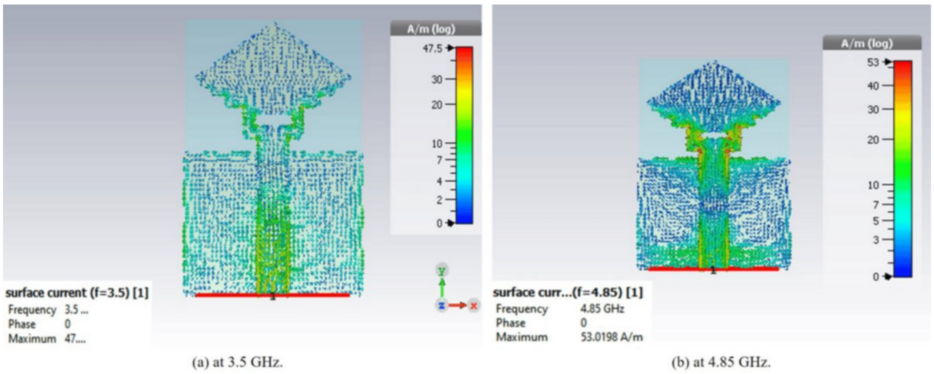

FIGURE 7: Surface current distribution of the proposed antenna

Radiation Pattern

The antenna's emitted energy is characterized by its radiation pattern. The farfield electric field (E-field) radiation patterns of the proposed antenna at phi = 0° and 90° are presented in Figure 8 for the resonant frequencies of 3.5 GHz. Figure 9 shows the radiation pattern of the antenna at 4.85 GHz for phi = 0° and 90°. The omnidirectional behavior of the antenna's radiation patterns at 3.5 GHz and 4.85 GHz suggests that it is an excellent choice for WBAN applications. At 3.5 GHz, the main lobe magnitudes are observed to be 17.1 dBV/m and 17.4 dBV/m, the main lobe directions are 180° and 167°, for phi = 0° (co-polarization) and 90° (cross polarization), respectively (Figure 8). From Figure 9, it is observed that the main lobe magnitudes are observed to be 15.6 dBV/m and 17.6 dBV/m, the main lobe directions are 180° and 146°, angular width (3dB) of 173° and 78.7°, and side lobe levels are −3.8 dB and −3.9 dB for phi = 0° and 90°, respectively.

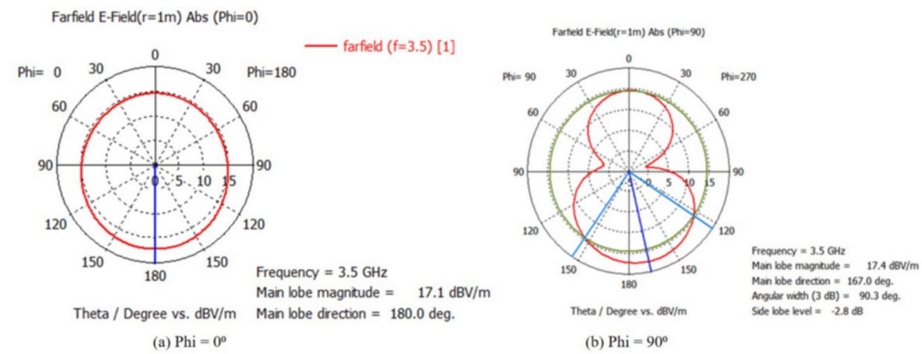

FIGURE 8: 2D farfield E-field radiation pattern of the proposed antenna at 3.5 GHz for (a) phi = 0 and (b) phi = 90°

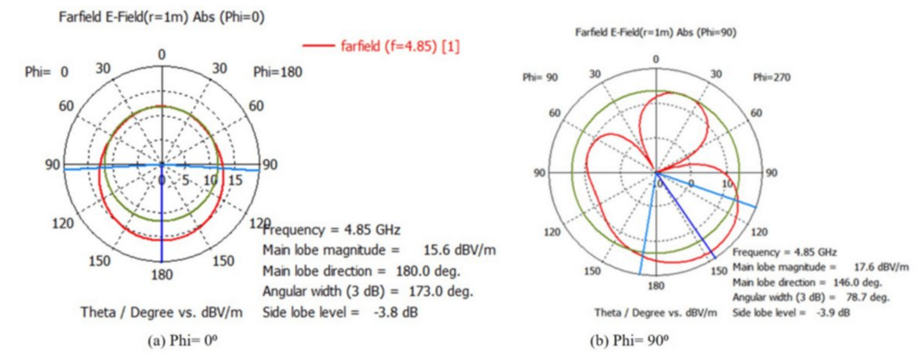

FIGURE 9: 2D farfield E-field radiation pattern of the proposed antenna at 4.85 GHz for (a) phi = 0° and (b) phi = 90°

On-body simulation results

The human tissues are lossy at higher frequencies. Due to wearable antennas operating in close proximity to the human body, the interaction between the antenna and human body tissues, as well as the impact on antenna performance parameters, is a significant consideration. Three tissue layers in a human body phantom were used to investigate the effects of human body reciprocity with the antenna. The phantom's dimensions are 40 × 30 × 8 mm^3. The phantom is composed of three layers: skin, fat, and muscular tissues with thicknesses of 1 mm, 3 mm, and 4 mm. The air gap between ground structure and skin is taken as 1 mm. Table *2* shows the relative permittivity, conductivity, and loss tangent at frequencies of 3.5 GHz and 4.85 GHz.

The CST software is used to create a body phantom model as shown in Figure *10a*. By using reports presented in [19,20], the properties of skin, fat, and muscle tissue layers are determined within the antenna's operating range of 2.53 to 5.81 GHz. Table *2* presents the derived electrical characteristics used to calculate SAR at the resonant peaks of 3.5 and 4.85 GHz of the antenna under the on-body condition.

Name of Tissue	Frequency (GHz)	Permittivity (ϵ_r)	Conductivity σ (s/m)	Loss Tangent	Mass density (kg/m^3)
Skin (dry)	3.5	37.005	2.0249	0.28103	1109
	4.85	35.896	2.9455	0.30412	
Fat	3.5	5.1739	0.15553	0.15439	911
	4.85	5.0433	0.23299	0.17122	
Muscle	3.5	51.444	2.5575	0.25533	1090
	4.85	49.735		0.28926	

TABLE 2: Electrical characteristics of tissue layers

Return loss (S11)

Figures *10b* shows the return loss (S11) of the proposed antenna. The return loss value under the on-body condition is higher than the off-body condition, although it is still significantly lower than −10 dB. The higher return loss is observed as a result of poor impedance matching caused by the body's reactive loading. When the antenna is placed very close to the body, its input impedance might be changed due to the fringing effect, which might change the effective width of the antenna structure and shift the resonant frequency. The off-body higher resonant peak at 4.85 GHz has shifted to a lower frequency.

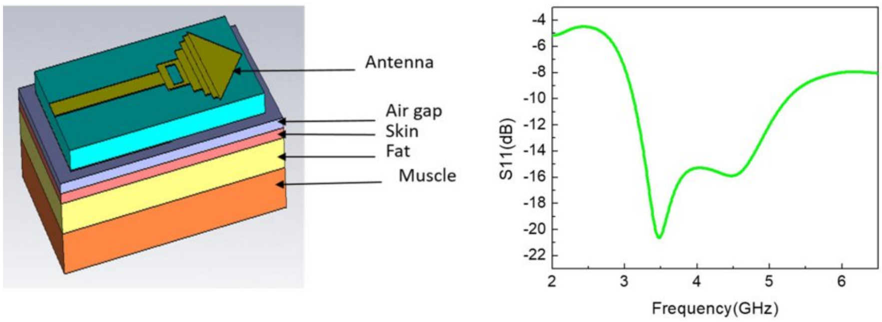

(a) Human body phantom model. (b) Return loss (S11) Vs. frequency.

FIGURE 10: On-body simulation results: (a) Phantom model and (b) Return loss

Gain

As the antenna is designed to operate at 3.5 GHz and 4.85 GHz, the analysis of gain, directivity, and efficiency is still done for those frequencies. Figure *11a* and b show the 3D farfield gain of the proposed antenna at the resonant frequencies on the human body phantom model. The results demonstrate that the antenna possesses necessary amount of gain for wireless transmission. The phantom's tissue layers may have absorbed electromagnetic energy at the operating frequency, as the gain for both resonant frequencies reduced in magnitude. As seen from the figure, the magnitudes of the obtained maximum gain are −0.7233 dB and −3.326 dB while the radiation efficiencies are −5.784 dB (26.40%) and −9.718 dB (10.88 %) at 3.5 GHz and 4.85 GHz, respectively.

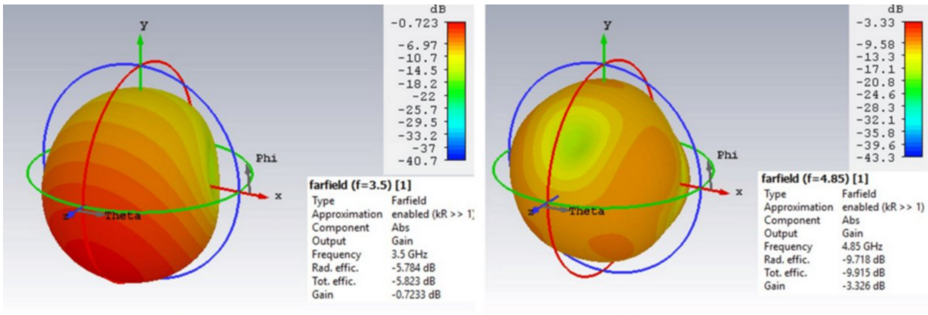

(a) Gain at 3.5 GHz. (b) Gain at 4.85 GHz.

FIGURE 11: Designed antenna farfield gain when placed on phantom

Radiation Pattern

The 2D polar plots of the simulated radiation farfield E-field patterns of the proposed antenna at 3.5 for for phi = 0° and 90° over the human body phantom model are shown in Figure *12*. Figure *13* shows the radiation pattern of the antenna at 4.85 GHz for phi = 0° and 90°. At 3.5 GHz, the main lobe magnitudes are observed to be −2.87 dBV/m and 14 dBV/m, the main lobe directions are 0 and 45 degrees, and 3dB angular beam widths are 102.4° and 45°, for phi = 0° and 90°, respectively.

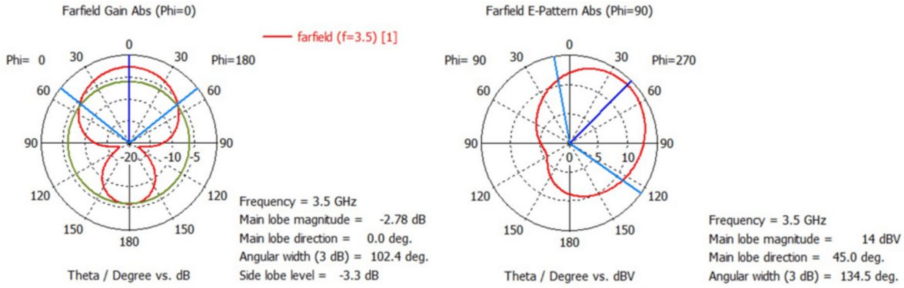

(a) Phi = 0° (b) Phi = 90°

FIGURE 12: 2D farfield E-field radiation pattern of the proposed antenna at 3.5 GHz for (a) phi = 0 and (b) phi = 90°

From Figure *13*, it is observed that the main lobe magnitudes are observed to be −5.32 dBV/m and 11.2 dBV/m, the main lobe directions are 180° and 156°, angular width (3dB) of 58.2° and 61.6°, and side lobe levels are −3.8 dB and −5.8 dB for phi = 0° and 90°, respectively.

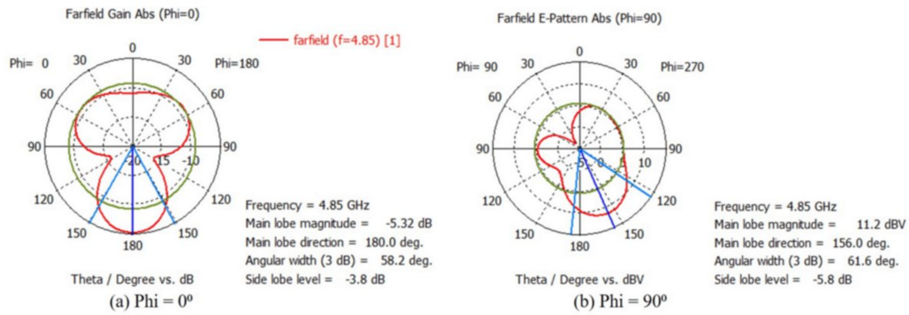

FIGURE 13: 2D farfield E-field radiation pattern of the proposed antenna at 4.85 GHz for (b) phi = 0 and (b) phi = 90°

Bending analysis

Since the proposed PDMS-based flexible antenna is designed to be attached to the human arm, some deformation of the antenna structure is to be predicted. Since adult and kid human arm sizes vary, four distinct bending situations (0°, 10°, 30°, and 40°) were chosen for analysis. The antenna bent was created and simulated with CST software, using a model of the human arm on which the antenna would be placed and bent. Figure *14* depicts the simulated reflection coefficient, S11, of the proposed antenna under flat and three bend conditions. With an increase in antenna bending degrees, it has been observed that the off-body resonance peak at 3.5 GHz (at 0 degrees of bending or flat condition) shifts toward a lower frequency. This shift may be caused by the antenna's changing structure in the bent form, which has an impact on the flow of surface current. These results are consistent with other studies in bending conditions [21,22]. The off-body higher resonance peak at 4.85 GHz has been observed to be shifted toward the higher frequency with an increase in degrees of antenna bending. However, the proposed antenna in bending conditions remains to operate within the specified frequency BW, although there is a shifting in frequency of its resonant peaks.

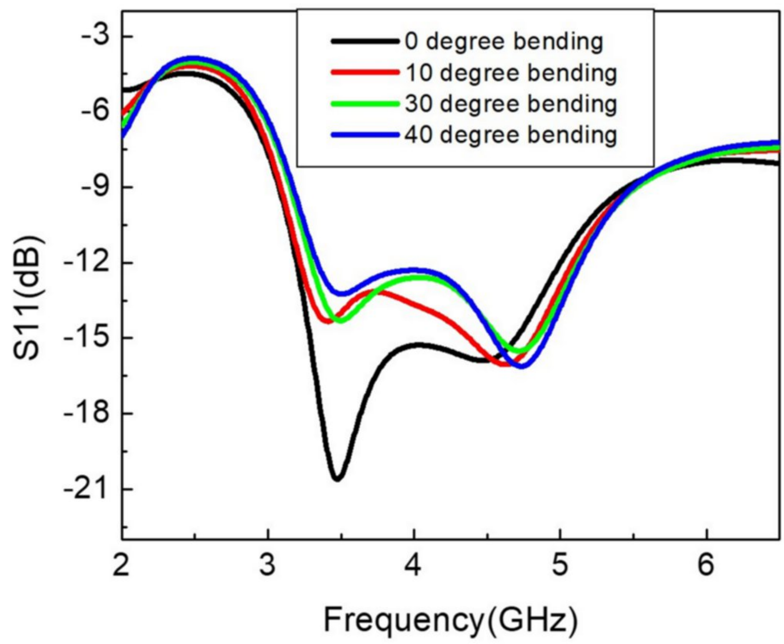

FIGURE 14: Return loss vs. frequency of the proposed antenna under bending

SAR analysis

The SAR measures the amount of EM energy absorbed per unit mass of the human body. The radiation from the designed antenna toward the human body must be controlled. The maximum safe limit of SAR defined by the US Federal Communications Commission (FCC) authority as 1.6 W/kg for 1 g of biological tissue, and by the European International Commission on Non-Ionizing Radiation Protection agency as 2 W/kg for 10 gm of tissue. In the present work, the SAR value is measured over 1 g of tissue using a three-layer flat body phantom model that is created with the dimensions of 40 × 30 × 8 mm^3. Input power of 1 mW is applied in CST to measure the SAR at the 3.5 GHz and 4.85 GHz resonant frequencies. The obtained SAR values are depicted in Figure *15*. The maximum SAR values of 0.134 W/kg at 3.5 GHz and 0.175 W/kg at 4.85 GHz are observed, which are much lower than the safe limit defined by the US FCC authority.

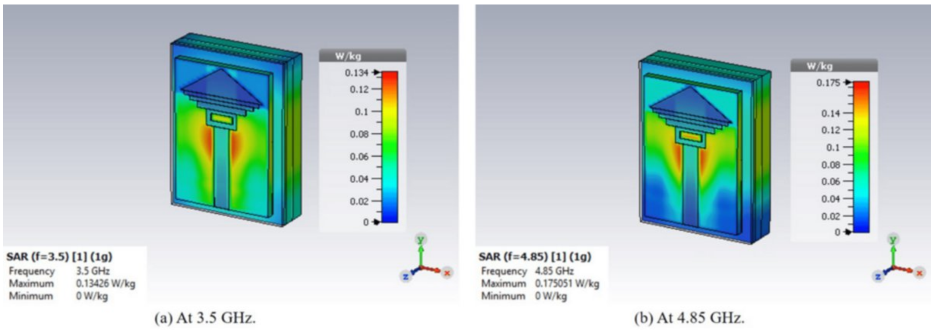

FIGURE 15: SAR analysis of the designed antenna at (a) 3.5 GHz and (b) 4.85 GHz

SAR, Specific Absorption Rate

Discussion

Comparative studies

A comparison of the performance of the proposed antenna with some other existing antennas published in earlier studies is tabulated in Table *3*. The table makes it clear that the proposed antenna is smaller and offers a larger operational BW with acceptable gain and efficiency. The proposed antenna has lower SAR values than other existing antennas. Using slots on triangular patch plane and defected ground structures (DGS) in the designed patch antennas can significantly enhance performance by improving BW, gain, and reducing unwanted radiation. Slots, particularly when strategically placed on the patch itself or the ground plane, can broaden the antenna's impedance BW, allowing it to operate over a wider range of frequencies. DGS, on the other hand, can increase gain, reduce cross-polarization, and minimize the impact of surface waves, ultimately improving the antenna's efficiency and performance. The proposed design incorporates a rectangular slot on a parallel bar of the patch plane, which has not been utilized in previous studies, and another slot on the partial ground plane. Combination of these slots and partial ground structure helps in improving impedance matching by providing smaller return losses. Moreover, the proposed antenna is smaller in size, has lower weight, and provides excellent impedance matching with a return loss value of less than −10 dB. The frequencies at which the antenna resonates are 4.85 GHz and 3.5 GHz and it operates within the frequency range of 2.53 GHz to 5.81 GHz, yielding a large BW of 3.28 GHz.

The antenna's primary operating frequency is 3.5 GHz; however, it also performs excellently at a higher frequency of 4.85 GHz. For 1 g of tissue, both the on-body analysis and the SAR analysis are carried out. The maximum SAR values obtained at the resonant frequencies are under the safety limit of 1.6 W/kg. The antenna offers a wide BW that covers the most popular lower 5G, WiMAX, WiFi, and ISM band applications. The realization of wide BW, good impedance matching, and low SAR values under the on-body condition make the designed antenna a good choice for future wearable electronic applications.

Ref. No.	Substrate Material/Permittivity	Antenna Size (L × W × h) mm^3	Bandwidth (GHz)	Gain (dBi)	Off-body/ On-body Efficiency (%)	SAR (W/kg)
[23]	Photopaper/3.2	40 × 30 × 0.27	3	3.48	84.35/12	1.53 (1 g) & 1.93 (10 g)
[24]	Polyester/2.8	135 × 50 × 47.5	0.35	8.53	NR	0.0698 (10 g)
[25]	RT/duroid 5880/2.2	68 × 38 × 1.57	2.45	6.88	NR	0.244 (1 g)
[26]	Wool felt/1.2	81 × 81 × 2	2.28-2.64	7.3	70/NR	0.23 (10 g) & 0.554 (1 g)
[27]	Rogers RO3003/3	62 × 42 × 4	2.36-2.4	6.2	NR	0.79 (1 g)
[28]	Polyimide/3.5	72 × 72 × 1.5	2.45 & 5.8	5.2 & 7.7	82.3/12.9 82.4/31.5	0.52.48 (1 g) @ 2.45 GHz & 0.7 (1 g) @ 5.8 GHz
[29]	Jeans fabric/1.9	72 × 71 × 1	0.03	1.7	23.1/18.6	0.0093 (1 g) & 0.025 (10 g)
[30]	FR-4/4.3	62 × 43 × 1.67	0.11	0.86	53/46	0.44 (1 g)
[31]	PDMS-AgNWs/2.8	50 × 50 × 5.5	2.4-2.6	2.4	79/68	0.18 (1 g)
[32]	PDMS/2.7	67 × 44 × 1.886	>13	6.76 dB	NR	1.482 (1 g)
This work	PDMS/2.74	35 × 25 × 2	3.28	2.58 dB	78.59/NR	0.134 (1 g) @ 3.5 GHz & 0.175 (1 g) @ 4.85 GHz

TABLE 3: Performance comparison of the proposed antenna with the previous work

NR, not reported; PDMS, polydimethylsiloxane

Conclusions

A wideband flexible compact microstrip patch antenna has been designed and simulated on a PDMS polymer substrate in this study for wearable electronic applications. The proposed antenna is made up of a patch, PDMS substrate, partial ground and a microstrip feed line, providing a net optimized dimension of 35 × 25 × 2 mm^3. The antenna's operating BW is increased by the incorporation of rectangular slots on the patch plane and partial ground plane. The proposed antenna resonates at two frequencies of 3.5 GHz and 4.85 GHz, operates within the 2.53-5.81 GHz range with a huge BW of 3.28 GHz, and a maximum radiation efficiency of 85.25%. This wide frequency range of operation covers the most popular lower 5G, WiMAX, WiFi, and ISM band applications. The performance parameters of the antenna have been evaluated and analyzed numerically under the off-body and on-body conditions and compared with the results obtained in earlier studies. Under the off-body condition, the antenna resonates at 3.50 GHz with return loss, VSWR, gain, directivity, surface current density, and radiation efficiency of −45.38 dB, 1.01, 2.58 dB, 3.62 dBi, 47.5 A/m, 78.59%, respectively. The antenna resonates at 4.85 GHz with return loss −27.53 dB, VSWR of 1.08, gain, directivity, surface current density and radiation efficiency of 2.8 dB, 4.46 dBi, 53 A/m, and 68.21%, respectively. Furthermore, when the antenna was placed on the human body phantom model, reasonable performance at both the resonant frequencies was obtained. The bending analysis also shows rational results. Moreover, from the SAR analysis, the obtained maximum SAR values of 0.134 W/kg at 3.5 GHz and 0.175 W/kg at 4.85 GHz at 1 g of tissue proved the proposed antenna satisfy the recommended safety constraints of less than 1.6 W/kg. The designed PDMS based flexible, small size, low weight, transparent slotted patch antenna shows convincing performance under both the off-body and on-body conditions, which makes it suitable for wideband wearable applications.

In future research, experiments will be conducted to validate key performance metrics under the off-body and on-body conditions with the fabrication and real-world testing of the antenna's performance to ensure its simulated performance and robustness. The S-parameter, VSWR, BW, gain, efficiency, and SAR data will be validated with the addition of the fabrication and experimental measurement work. Additionally, a more complex and realistic phantom model will be used in future work for strengthen the on-body analysis. A more comprehensive analysis will be done with various bending radii and directions to provide a more complete picture of the antenna's performance under deformation.

Additional Information

Author Contributions

All authors have reviewed the final version to be published and agreed to be accountable for all aspects of the work.

Concept and design: Abu Zafor Muhammad Touhidul Islam, Md. Mehedi Hasan

Acquisition, analysis, or interpretation of data: Abu Zafor Muhammad Touhidul Islam, Md. Mehedi Hasan

Critical review of the manuscript for important intellectual content: Abu Zafor Muhammad Touhidul Islam, Md. Mehedi Hasan

Supervision: Abu Zafor Muhammad Touhidul Islam

Drafting of the manuscript: Md. Mehedi Hasan

Disclosures

Human subjects: All authors have confirmed that this study did not involve human participants or tissue. **Animal subjects:** All authors have confirmed that this study did not involve animal subjects or tissue. **Conflicts of interest:** In compliance with the ICMJE uniform disclosure form, all authors declare the following: **Payment/services info:** All authors have declared that no financial support was received from any organization for the submitted work. **Financial relationships:** All authors have declared that they have no financial relationships at present or within the previous three years with any organizations that might have an interest in the submitted work. **Other relationships:** All authors have declared that there are no other relationships or activities that could appear to have influenced the submitted work.

References

1. Paracha KN, Rahim SKA, Soh PJ, et al.: Wearable antennas: a review of materials, structures, and innovative features for autonomous communication and sensing. IEEE Access. 2019, 7:56694-712. 10.1109/ACCESS.2019.2909146
2. Jiang ZH, Gregory MD, Werner DH: Design and experimental investigation of a compact circularly polarized integrated filtering antenna for wearable biotelemetric devices. IEEE Transactions on Biomedical Circuits and Systems. 2016, 10:328-38. 10.1109/TBCAS.2015.2438551
3. Björninen T, Yang F: Low-profile head-worn antenna with a monopole-like radiation pattern. IEEE Antennas and Wireless Propagation Letters. 2016, 15:794-97. 10.1109/LAWP.2015.2475158
4. Ali SM, Sovuthy C, Imran MA, Socheatra S, Abbasi QH, Abidin ZZ: Recent advances of wearable antennas in materials, fabrication methods, designs, and their applications: state-of-the-art. Micromachines. 2020, 11:888. 10.3390/mi11100888
5. Suma MN, Bybi PC, Mohanan P: A wideband printed monopole antenna for 2.4-GHz WLAN applications. Microwave and Optical Technology Letters. 2006, 48:871-73. 10.1002/mop.21503
6. Arif A, Zubair M, Ali M, Khan MU, Mehmood MQ: A compact, low-profile fractal antenna for wearable on-body WBAN applications. IEEE Antennas and Wireless Propagation Letters. 2019, 18:981-85. 10.1109/LAWP.2019.2906829
7. Soh PJ, Vandenbosch GAE, Ooi SL, Rais NHM: Design of a broadband all-textile slotted PIFA. IEEE Transactions on Antennas and Propagation. 2012, 60:379-84. 10.1109/TAP.2011.2167950
8. Nechayev YI, Hall PS, Hu ZH: Characterisation of narrowband communication channels on the human body at 2.45 GHz. IET Microwaves Antennas & Propagation. 2010, 4:722-32. 10.1049/iet-map.2009.0094
9. Kim S, Ren YJ, Lee H, Rida A, Nikolaou S, Tentzeris MM: Monopole antenna with inkjet-printed EBG array on paper substrate for wearable applications. IEEE Antennas and Wireless Propagation Letters. 2012, 11:663-66. 10.1109/LAWP.2012.2203291
10. Alomainy A, Hao Y, Owadally A, Parini CG, Nechayev Y, Constantinou CC, Hall PS: Statistical analysis and performance evaluation for on-body radio propagation with microstrip patch antennas. IEEE Transactions on Antennas and Propagation. 2007, 55:245-48. 10.1109/TAP.2006.888462
11. Li H, Sun S, Wang B, Wu F: Design of compact single-layer textile MIMO antenna for wearable applications. IEEE Transactions on Antennas and Propagation. 2018, 66:3136-41. 10.1109/TAP.2018.2811844
12. Velan S, Sundarsingh EF, Kanagasabai M, Sarma AK, Raviteja C, Sivasamy R: Dual-band EBG integrated monopole antenna deploying fractal geometry for wearable applications. IEEE Antennas and Wireless Propagation Letters. 2015, 14:249-52. 10.1109/LAWP.2014.2360710
13. Mobashsher AT, Abbosh AM: Performance of directional and omnidirectional antennas in wideband head imaging. IEEE Antennas and Wireless Propagation Letters. 2016, 15:1618-21. 10.1109/LAWP.2016.2519527
14. Sayem ASM, Simorangkir RBVB, Esselle KP, Hashmi RM: Feasibility study of PDMS embedded transparent conductive fabric for the realization of transparent flexible antennas. 13th European Conference on Antennas and Propagation (EuCAP), Krakow, Poland. 2019, 1-4.
15. Simorangkir RBVB, Yang Y, Hashmi RM, Björninen T, Esselle KP, Ukkonen L: Polydimethylsiloxane-embedded conductive fabric: characterization and application for realization of robust passive and active flexible wearable antennas. IEEE Access. 2018, 6:48102-112. 10.1109/ACCESS.2018.2867696
16. Alqadami ASM, Mohammed B, Bialkowski KS, Vandenbosch GAE: Assessment of PDMS Technology in a MIMO Antenna Array. IEEE Antennas and Wireless Propagation Letters. 2016, 15:1939-42. 10.1109/LAWP.2015.2513960
17. Joshi R, Constantinides C, Podilchak SK, Ramli MN, Lago H, Soh PJ: Robust and compact PDMS antennas for search and rescue operations and emergency communications. 12th European Conference on Antennas and Propagation (EuCAP 2018). 2018, 1-5. 10.1049/cp.2018.0975

18. Hassan WHW, Li NY, Azize AM, Zakaria Z, Shairi NA, Hamid MHA: Simulation on wideband antenna based on Polydimethylsiloxane (PDMS) for medical imaging application. Journal of Physics Conference Series. 2020, 1502:012008. 10.1088/1742-6596/1502/1/012008
19. Hasgall PA, Di Gennaro F, Baumgartner C, et al.: IT'IS database for thermal and electromagnetic parameters of biological tissues. Version 4.1. 2022, 10.13099/VIP21000-04-1
20. IFAC-CNR Report: An Internet resource for the calculation of the dielectric properties of body tissues in the frequency range 10 Hz - 100 GHz. (1997). Accessed: May 20, 2024: http://niremf.ifac.cnr.it/tissprop/.
21. Mersani A, Osman L, Ribero JM: Effect of bending on the characteristics of a coplanar textile antenna. 18th Mediterranean Microwave Symposium (MMS), Istanbul, Turkey. 2018, 255-57. 10.1109/MMS.2018.8612049
22. Salleh SM, Ain MF, Ahmad Z, Abidin ISZ, Isa CMNC: Development of stretchable and bendable polymer wearable antenna for 5G applications. eXPRESS Polymer Letters. 2022, 16:1267-79.
23. Jabbar A, Zubair M, Naveed MA, Mehmood MQ, Massoud Y: A photopaper-based low-cost, wideband wearable antenna for wireless body area network applications. IET Microwaves Antennas & Propagation. 2022, 16:962-70. 10.1049/mia2.12313
24. Abirami BS, Sundarsingh EF: EBG-backed flexible printed yagi-uda antenna for on-body communication. IEEE Transactions on Antennas and Propagation. 2017, 65:3762-65. 10.1109/tap.2017.2705224
25. Abbasi MAB, Nikolaou SS, Antoniades MA, Stevanović MN, Vryonides P: Compact EBG-backed planar monopole for BAN wearable applications. IEEE Transactions on Antennas and Propagation. 2017, 65:453-63. 10.1109/TAP.2016.2635588
26. Gao GP, Hu B, Wang SF, et al.: Wearable circular ring slot antenna with EBG structure for wireless body area network. IEEE Antennas and Wireless Propagation Letters. 2018, 17:434-37. 10.1109/LAWP.2018.2794061
27. Jiang ZH, Brocker DE, Sieber PE, et al.: A compact, low-profile metasurface-enabled antenna for wearable medical body-area network devices. IEEE Transactions on Antennas and Propagation. 2014, 62:4021-30. 10.1109/TAP.2014.2327650
28. Wang M, Yang Z, Wu J, et al.: Investigation of SAR reduction using flexible antenna with metamaterial structure in wireless body area network. IEEE Transactions on Antennas and Propagation. 2018, 66:3076-86. 10.1109/TAP.2018.2820733
29. Gil I, Fernández-García R: Wearable GPS patch antenna on jeans fabric. Progress in Electromagnetic Research Symposium (PIERS). Shanghai, China; 2016. 2019-22. 10.1109/PIERS.2016.7734859
30. Ali SM, Jeoti V, Saeidi T, Wen WP: Design of compact microstrip patch antenna for WBAN applications at ISM 2.4 GHz. Indonesian Journal of Electrical Engineering and Computer Science. 2019, 15:10.11591/ijeecs.v15.i3.pp1509-1516
31. Jiang ZH, Cui Z, Yue T, Zhu Y, Werner DH: Compact, highly efficient, and fully flexible circularly polarized antenna enabled by silver nanowires for wireless body-area networks. IEEE Transactions on Biomedical Circuits and Systems. 2017, 11:920-32. 10.1109/tbcas.2017.2671841
32. Janapala DK, Nesasudha M, Neebha TM, Kumar R: Design and development of flexible PDMS antenna for UWB-WBAN applications. Wireless Personal Communications. 2021, 122:3467-83. 10.1007/s11277-021-09095-7